Explicit formulas for effective piezoelectric coefficients of ferroelectric 0–3 composites based on effective medium theory

C. K. Wong[a)]
Department of Applied Physics, The Hong Kong Polytechnic University, Hong Kong, People's Republic of China

Y. M. Poon
Department of Applied Physics and Materials Research Center, The Hong Kong Polytechnic University, Hong Kong, People's Republic of China

F. G. Shin
Department of Applied Physics, Materials Research Center and Center for Smart Materials, The Hong Kong Polytechnic University, Hong Kong, People's Republic of China

(Received 13 June 2002; accepted 8 October 2002)

Explicit formulas were derived for the effective piezoelectric stress coefficients of a 0–3 composite of ferroelectric spherical particles in a ferroelectric matrix which were then combined to give the more commonly used strain coefficients. Assuming that the elastic stiffness of the inclusion phase is sufficiently larger than that of the matrix phase, the previously derived explicit expressions for the case of a low volume concentration of inclusion particles [C. K. Wong, Y. M. Poon, and F. G. Shin, Ferroelectrics **264**, 39 (2001); J. Appl. Phys. **90**, 4690 (2001)] were ''transformed'' analytically by an effective medium theory (EMT) with appropriate approximations, to suit the case of a more concentrated suspension. Predictions of the EMT expressions were compared with the experimental values of composites of lead zirconate titanate ceramic particles dispersed in polyvinylidene fluoride and polyvinylidene fluoride-trifluoroethylene copolymer, reported by Furukawa [IEEE Trans. Electr. Insul. **24**, 375 (1989)] and by Ng *et al.* [IEEE Trans. Ultrason. Ferroelectr. Freq. Control **47**, 1308 (2000)] respectively. Fairly good agreement was obtained. Comparisons with other predictions, including the predictions given by numerically solving the EMT scheme, were also made. It was found that the analytic and numeric EMT schemes agreed with each other very well for an inclusion of volume fraction not exceeding 60%. © *2003 American Institute of Physics.*
[DOI: 10.1063/1.1524720]

I. INTRODUCTION

There have been many theories and models of different approaches proposed for the prediction of the effective piezoelectric properties of multiphase heterogeneous composite materials.[1–11] Some results are simple, elegant expressions derived from simplified approaches. In the rigorous and often more complicated approaches, difficult numerical computation schemes must invariably be employed to get predictions of the effective properties. In our previous articles,[6,7] we aimed at obtaining analytical expressions for the effective piezoelectric coefficients and derived some explicit expressions for the effective piezoelectric strain coefficients (d_{31}, d_{33} and d_h) for ferroelectric 0–3 composites when the volume fraction of the inclusion phase is small.[6] Then the dilute suspension results were re-expressed to involve the effective dielectric and elastic properties of the composite,[7] which could be measured or evaluated by some dielectric and elastic formulas applicable to higher volume fractions of inclusions. Consequently, the predictions of the effective piezoelectric coefficients given by such a method are not so limited to low volume fraction of inclusions.

For higher inclusion volume fractions, the derivation of accurate effective piezoelectric properties of composite materials that starts from electrostatics and elasticity or from energy considerations can be quite complicated. Effective medium theories are approaches that allow results for higher inclusion volume fraction to be obtained from dilute limit results. They define an ''effective'' medium systematically to phenomenologically tackle the originally complex problem of inclusion interactions. In fact, there exist many effective medium type theories in the literature. A well-known example is the effective medium approximation (EMA),[12,13] which is a simple approach of wide applicability, especially in percolating systems.[14,15] For the piezoelectric composite problems, Nan,[8] Nan *et al.*[9,10] and Zewdie[11] used effective medium theories to study the piezoelectric property of 0–3 composites and their theories are based on the EMA. In contrast, Shin *et al.*[16–19] developed effective medium theory (EMT) which came closer to the scheme of differential effective medium (DEM) theory,[20] but the framework is simpler and more straightforward.[21] In this article, we attempt to extend the effective medium theory reported in Refs. 16–19 to piezoelectric composite problems. Originally, the formulation of this theory was for the effective dielectric properties of binary mixtures. Later on, this formulation was extended to the prediction of elastic properties of isotropic composites

a)Electronic mail: wongck.a@polyu.edu.hk

whose EMT equations involve two substrate variables.[19,21] A physical property of a composite may depend on a number of properties of the substrate (i.e., the matrix phase) which are taken as variables, called substrate variables, as well as the inclusion volume fraction. In principle, the EMT would not be limited only to dielectric or elastic properties of the composites. It is readily extensible to cases of several substrate variables. Piezoelectric problems always couple the equations of electrostatics with elasticity and, therefore, they involve at least four substrate variables.

The predictions given by our adopted EMT are reasonably good as demonstrated by previous work[16–19,21] on dielectric and elastic properties of binary composites. However, it is not easy to obtain analytical results since EMT involves solving of partial differential equations. For example, Au *et al.*[21] gave implicit expressions for the effective shear modulus and Poisson ratio in the limiting case of composites with rigid spherical inclusions. The general case of spherical inclusions cannot be solved analytically to get simple formulas.

In this article, we have successfully obtained explicit expressions for the effective piezoelectric stress coefficients (*e* coefficients) under the assumption that the shear and bulk moduli of the inclusion phase are much larger than the corresponding properties of the matrix phase, i.e., inclusions are elastically rigid. In this case, analytic solutions for the differential equations of EMT are greatly simplified and tractable. [In comparison, if one tried to solve the effective strain coefficients (*d* coefficients) directly following the same footsteps and rigidity assumption, then the resulting differential equations would become substantially more complicated.] The results were then used to calculate the effective piezoelectric *d* coefficients. Manipulations of equations were made before applying the rigidity assumption and as a result notable disagreement with the numeric EMT scheme (without the assumption of elastically rigid inclusions) occurs only beyond 60% of the inclusion volume fraction. Experimental data[22] of d_{31} for lead zirconate titanate/polyvinylidene fluoride (PZT/PVDF), and experimental data[23] of d_{33} for a PZT/vinylidene fluoride-trifluoroethylene [PZT/P(VDF-TrFE)] copolymer for different poling conditions are used for comparison with our theoretical predictions, along with the predictions given by Nan and Weng.[10]

II. THEORY

To calculate the effective piezoelectric d_{31} and d_{33} coefficients of a 0–3 composite, we will first derive the e_h ($\equiv e_{33}+2e_{31}$) and e_s($\equiv e_{33}-e_{31}$) coefficients which correspond to hydrostatic and shear loading conditions, respectively. Then the results can be combined through relations

$$d_{\gamma\alpha}=e_{\gamma\beta}s_{\beta\alpha}, \qquad e_{\gamma\alpha}=d_{\gamma\beta}c_{\beta\alpha}, \tag{1}$$

to obtain expressions for the e_{31}, e_{33}, d_{31}, d_{33} and d_h ($\equiv d_{33}+2d_{31}$) coefficients. $s_{\beta\alpha}$ and $c_{\beta\alpha}$ denote elastic compliance and stiffness coefficients, respectively. Subscripts $\gamma=1, 2, 3$ and $\alpha, \beta=1,\Lambda,6$. These elastic coefficients of the composites can be either calculated from models of composite elastic properties or adopted from experimental results.

A. Expressions for effective piezoelectric *e* coefficients in the dilute limit

In a previous paper,[7] we have derived the volume-averaged electric displacement (directed along the *Z* direction) and piezoelectric coefficients of the composite as

$$\langle D_3\rangle=\varepsilon\langle E_3\rangle+d_{31}\langle\sigma_{xx}\rangle+d_{32}\langle\sigma_{yy}\rangle+d_{33}\langle\sigma_{zz}\rangle, \tag{2}$$

where

$$d_{31}=d_{32}=\phi L_E\{(L_T^{\perp}+L_T^{\parallel})d_{31i}+L_T^{\perp}d_{33i}\} +(1-\phi)\overline{L}_E\{(\overline{L}_T^{\perp}+\overline{L}_T^{\parallel})d_{31m}+\overline{L}_T^{\perp}d_{33m}\}, \tag{3}$$

$$d_{33}=\phi L_E\{2L_T^{\perp}d_{31i}+L_T^{\parallel}d_{33i}\} +(1-\phi)\overline{L}_E\{2\overline{L}_T^{\perp}d_{31m}+\overline{L}_T^{\parallel}d_{33m}\}, \tag{4}$$

and

$$d_h=2d_{31}+d_{33}=\phi L_E L_T^h d_{hi}+(1-\phi)\overline{L}_E\overline{L}_T^h d_{hm}, \tag{5}$$

$$L_E=\frac{1}{\phi}\frac{\varepsilon-\varepsilon_m}{\varepsilon_i-\varepsilon_m}, \quad L_T^{\perp}=\frac{1}{\phi}\left\{\frac{1}{3}\frac{k^{-1}-k_m^{-1}}{k_i^{-1}-k_m^{-1}}-\frac{1}{3}\frac{\mu^{-1}-\mu_m^{-1}}{\mu_i^{-1}-\mu_m^{-1}}\right\}, \quad L_T^{\parallel}=\frac{1}{\phi}\left\{\frac{1}{3}\frac{k^{-1}-k_m^{-1}}{k_i^{-1}-k_m^{-1}}+\frac{2}{3}\frac{\mu^{-1}-\mu_m^{-1}}{\mu_i^{-1}-\mu_m^{-1}}\right\}, \tag{6}$$

$$\overline{L}_E=(1-\phi L_E)/(1-\phi), \quad \overline{L}_T^{\perp}=-\phi L_T^{\perp}/(1-\phi), \quad \overline{L}_T^{\parallel}=(1-\phi L_T^{\parallel})/(1-\phi), \tag{7}$$

$$L_T^h=2L_T^{\perp}+L_T^{\parallel}, \quad \overline{L}_T^h=2\overline{L}_T^{\perp}+\overline{L}_T^{\parallel}=(1-\phi L_T^h)/(1-\phi), \tag{8}$$

where ε, k and μ denote permittivity, bulk modulus and shear modulus of the composite, respectively, ϕ is the volume fraction of the inclusion phase, while $\langle E_3\rangle$ and $\langle\sigma_{xx}\rangle$, $\langle\sigma_{yy}\rangle$, $\langle\sigma_{zz}\rangle$ are the volumetric average electric field and stresses, respectively. Subscripts *i* and *m* denote the inclusion and matrix, respectively. In the original reference,[7] L_T's in Eqs. (6) were cast in terms of the Young's moduli and Poisson ratio and were more robust.

By setting $\langle\sigma_{zz}\rangle=-\langle\sigma_{xx}\rangle\equiv\langle\sigma\rangle$ and $\langle\sigma_{yy}\rangle=0$ which corresponds to the pure shear loading condition in Eq. (2), we can define $d_s\equiv d_{33}-d_{31}$ and obtain

$$d_s=\phi L_E L_T^s d_{si}+(1-\phi)\overline{L}_E\overline{L}_T^s d_{sm}, \tag{9}$$

where

$$L_T^s\equiv L_T^{\parallel}-L_T^{\perp}=(1/\phi)(\mu^{-1}-\mu_m^{-1})/(\mu_i^{-1}-\mu_m^{-1}), \quad \overline{L}_T^s\equiv\overline{L}_T^{\parallel}-\overline{L}_T^{\perp}=(1-\phi L_T^s)/(1-\phi). \tag{10}$$

The piezoelectric $e_h(\equiv e_{33}+2e_{31})$ and $e_s(\equiv e_{33}-e_{31})$ coefficients can be obtained from expressions of the *d* coefficients. From Eqs. (1), the relations $e_{31}=2(3k+\mu)d_{31}/3+(3k-2\mu)d_{33}/3$ and $e_{33}=2(3k-2\mu)d_{31}/3+(3k$

$+4\mu)d_{33}/3$ can be written for elastically isotropic materials. From this, we get $e_h=3kd_h$ and $e_s=2\mu d_s$. Expressions for the effective piezoelectric e_h and e_s coefficients are given by

$$e_h=\phi L_E L_S^h e_{hi}+(1-\phi)\overline{L}_E\overline{L}_S^h e_{hm},$$
$$e_s=\phi L_E L_S^s e_{si}+(1-\phi)\overline{L}_E\overline{L}_S^s e_{sm}, \tag{11}$$

where

$$L_S^h=\frac{1}{\phi}\frac{k-k_m}{k_i-k_m},$$
$$L_S^s=\frac{1}{\phi}\frac{\mu-\mu_m}{\mu_i-\mu_m}, \tag{12}$$

$$\overline{L}_S^h=(1-\phi L_S^h)/(1-\phi),$$
$$\overline{L}_S^s=(1-\phi L_S^s)/(1-\phi). \tag{13}$$

Expressions for the effective piezoelectric e_{31} and e_{33} coefficients can be written in the similar way. Equations (11) may be written in the form of

$$e=\phi L_E L_S e_i+(1-\phi)^{-1}(1-\phi L_E)(1-\phi L_S)e_m, \tag{14}$$

where

$$L_S=\frac{1}{\phi}\frac{c-c_m}{c_i-c_m}; \tag{15}$$

c is the bulk modulus k for $e=e_h$ or the shear modulus μ when $e=e_s$. Notice that Eq. (14) is much simpler than the corresponding expressions for d_{33} and d_{31} [Eqs. (3) and (4)]. Moreover, the effective e_h and e_s coefficients depend on three substrate variables only (versus on five variables for d_{31} and d_{33}), so we can appreciate the advantage of solving for e_h and e_s first via the use of EMT characteristic equations for this system and then obtain d_h, e_{31}, e_{33}, d_{31} and d_{33}.

B. Application of the EMT equations to solve for piezoelectric coefficients

The effective medium theory mentioned earlier has already been applied to dielectric and elastic property studies of binary mixtures and composites by Shin *et al.*[16–19,21] Following the same idea and steps, the extension of EMT to piezoelectric properties is essentially identical, but now more substrate variables are involved. Thus, following the effective medium arguments that lead to the effective elastic properties,[19,21] an additional first order partial differential equation is obtained for the piezoelectric problems at hand:

$$(1-\phi)\frac{\partial e}{\partial\phi}=\frac{\partial e}{\partial\varepsilon_m}\left[\frac{\partial\varepsilon}{\partial\phi}\right]_{\phi=0}+\frac{\partial e}{\partial c_m}\left[\frac{\partial c}{\partial\phi}\right]_{\phi=0}+\frac{\partial e}{\partial e_m}\left[\frac{\partial e}{\partial\phi}\right]_{\phi=0}. \tag{16}$$

The characteristic equation of Eq. (16) is

$$\frac{-d\phi}{1-\phi}=\frac{d\varepsilon_m}{[\partial\varepsilon/\partial\phi]_{\phi=0}}=\frac{dc_m}{[\partial c/\partial\phi]_{\phi=0}}=\frac{de_m}{[\partial e/\partial\phi]_{\phi=0}}. \tag{17}$$

When ϕ approaches zero, L_E and L_S in Eqs. (6) and (15) may be written as

$$L_E|_{\phi\to0}=\frac{1}{\varepsilon_i-\varepsilon_m}\lim_{\phi\to0}\frac{\varepsilon-\varepsilon_m}{\phi}=\frac{-d\ln(\varepsilon_i-\varepsilon_m)}{d\varepsilon_m}\left[\frac{\partial\varepsilon}{\partial\phi}\right]_{\phi=0},$$
$$L_S|_{\phi\to0}=\frac{1}{c_i-c_m}\lim_{\phi\to0}\frac{c-c_m}{\phi}=\frac{-d\ln(c_i-c_m)}{dc_m}\left[\frac{\partial c}{\partial\phi}\right]_{\phi=0}. \tag{18}$$

From Eq. (14), we can write $(e-e_m)/\phi=L_E L_S e_i+(1-L_E-L_S+\phi L_E L_S)e_m/(1-\phi)$. Hence

$$[\partial e/\partial\phi]_{\phi=0}=\lim_{\phi\to0}[(e-e_m)/\phi]=L_E|_{\phi\to0}L_S|_{\phi\to0}e_i+\{1-L_E|_{\phi\to0}-L_S|_{\phi\to0}\}e_m. \tag{19}$$

Using Eqs. (18) and (19), Eq. (17) becomes

$$\begin{aligned}\frac{d\ln(1-\phi)}{1}&=\frac{-d\ln(\varepsilon_i-\varepsilon_m)}{L_E|_{\phi\to0}}\\&=\frac{-d\ln(c_i-c_m)}{L_S|_{\phi\to0}}\\&=\frac{d\ln\{(1-\phi)(\varepsilon_i-\varepsilon_m)(c_i-c_m)\}}{1-L_E|_{\phi\to0}-L_S|_{\phi\to0}}\\&=\frac{de_m}{L_E|_{\phi\to0}L_S|_{\phi\to0}e_i+\{1-L_E|_{\phi\to0}-L_S|_{\phi\to0}\}e_m}.\end{aligned} \tag{20}$$

From Eq. (20), a differential equation results: $de_m/d\ln(1-\phi)=L_E|_{\phi\to0}L_S|_{\phi\to0}e_i+\{1-L_E|_{\phi\to0}-L_S|_{\phi\to0}\}e_m$. By using Eq. (20) again, this differential equation is rewritten as

$$\frac{d(e_m-e_i)}{d\ln(1-\phi)}=\frac{d\ln\{(1-\phi)(\varepsilon_i-\varepsilon_m)(c_i-c_m)\}}{d\ln(1-\phi)}(e_m-e_i)+(1-L_E|_{\phi\to0})(1-L_S|_{\phi\to0})e_i, \tag{21}$$

which is a first order linear equation in e_m-e_i. Upon integration, we obtain

$$\frac{e_m-e_i}{(1-\phi)(\varepsilon_i-\varepsilon_m)(c_i-c_m)}=\int\frac{(1-L_E|_{\phi\to0})(1-L_S|_{\phi\to0})e_i}{(1-\phi)(\varepsilon_i-\varepsilon_m)(c_i-c_m)}d\ln(1-\phi). \tag{22}$$

Making use of Eq. (20), we can rewrite it as

$$\frac{e_m-e_i}{(1-\phi)(\varepsilon_i-\varepsilon_m)(c_i-c_m)}=-e_i\int\frac{d[(1-\phi)^{-1}(\varepsilon_i-\varepsilon_m)^{-1}]d[(1-\phi)^{-1}(c_i-c_m)^{-1}]}{d[(1-\phi)^{-1}]}. \tag{23}$$

A first integral obtained from Eq. (17) and the Maxwell-Wagner formula[24] is (also see the Appendix):

$$S=(1-\phi)\frac{\varepsilon_i-\varepsilon_m}{\varepsilon_m^{1/3}}, \tag{24}$$

which gives the Bruggeman formula.[25] By substituting Eq. (24) into Eq. (23), we finally obtain

$$\frac{e_m-e_i}{(1-\phi)(\varepsilon_i-\varepsilon_m)(c_i-c_m)}=-e_i\int\frac{1}{\varepsilon_i+2\varepsilon_m}d\left[\frac{1}{(1-\phi)(c_i-c_m)}\right]. \tag{25}$$

The integral on the right-hand side involves variables ϕ, ε_m and c_m, and is difficult to evaluate exactly in this form. In order to obtain analytical results, some approximations would have to be employed. In this work we are mainly interested in piezoelectric composite systems in which ceramic particles are embedded in polymeric matrices. Normally in such cases $k_i \gg k_m$ and $\mu_i \gg \mu_m$. Care must be taken when we apply these approximations directly to the integral on the right-hand side of Eq. (25). Sometimes the approximated integral can deviate quite significantly from the numeric integration result (obtained by numeric integration without making the foregoing approximations) and the solution for the e coefficient then does not approach the correct limit at $\phi=1$. Therefore, guided by numeric integration, we perform integration by parts twice and get

$$\frac{e_m-e_i}{(1-\phi)(\varepsilon_i-\varepsilon_m)(c_i-c_m)}=-e_i\left\{\frac{\varepsilon_i+4\varepsilon_m}{(1-\phi)(\varepsilon_i+2\varepsilon_m)^2(c_i-c_m)}-2\int\varepsilon_m d\left[\frac{1}{(1-\phi)(\varepsilon_i+2\varepsilon_m)^2(c_i-c_m)}\right]\right\} \tag{26}$$

before we apply any approximations, which will be done below. Equation (26) seems to have extracted the most significant portion from the integral and smaller errors are introduced into the final result when we take approximations inside the integral to obtain closed form results.

C. Effective piezoelectric e coefficients

For derivation of the effective hydrostatic piezoelectric coefficient e_h, all e's in Eq. (26) are to be interpreted as e_h and all c values as bulk modulus k [cf. Eqs. (14) and (15)]. Many biphasic ferroelectric composites involve a ceramic inclusion and polymer matrix [e.g., PZT/P(VDF-TrFE)]. In such cases, we can take $k_i \gg k_m$, and the integral in Eq. (26) can be approximated to

$$I_h\equiv-2\int\varepsilon_m d\left[\frac{1}{(1-\phi)(\varepsilon_i+2\varepsilon_m)^2(k_i-k_m)}\right]\approx\frac{-2}{k_i}\int\varepsilon_m d\left[\frac{1}{(1-\phi)(\varepsilon_i+2\varepsilon_m)^2}\right], \tag{27}$$

where the subscript h denotes the hydrostatic loading condition. Making use of Eq. (24) and then integrating, the result is

$$I_h=\frac{-2}{Sk_i}\int\varepsilon_m d\left[\frac{\varepsilon_i-\varepsilon_m}{\varepsilon_m^{1/3}(\varepsilon_i+2\varepsilon_m)^2}\right]=\frac{\varepsilon_m^{2/3}}{Sk_i}\frac{\varepsilon_i+8\varepsilon_m}{(\varepsilon_i+2\varepsilon_m)^2}. \tag{28}$$

Substituting Eq. (24) into Eq. (28) to eliminate S, an approximate first integral is obtained from Eq. (26):

$$\Phi_h(\phi)=\frac{e_{hm}-e_{hi}}{(1-\phi)(\varepsilon_i-\varepsilon_m)(k_i-k_m)}+\frac{e_{hi}}{(1-\phi)(\varepsilon_i+2\varepsilon_m)^2}\times\left\{\frac{\varepsilon_i+4\varepsilon_m}{k_i-k_m}+\frac{(\varepsilon_i+8\varepsilon_m)\varepsilon_m}{(\varepsilon_i-\varepsilon_m)k_i}\right\}. \tag{29}$$

At $\phi=0$:

$$\Phi_h(0)=\frac{e_{hm}-e_{hi}}{(\varepsilon_i-\varepsilon_m)(k_i-k_m)}+\frac{e_{hi}}{(\varepsilon_i+2\varepsilon_m)^2}\times\left\{\frac{\varepsilon_i+4\varepsilon_m}{k_i-k_m}+\frac{(\varepsilon_i+8\varepsilon_m)\varepsilon_m}{(\varepsilon_i-\varepsilon_m)k_i}\right\}. \tag{30}$$

Thus for a general ϕ,

$$\frac{e_h-e_{hi}}{(\varepsilon_i-\varepsilon)(k_i-k)}+\frac{e_{hi}}{(\varepsilon_i+2\varepsilon)^2}\left\{\frac{\varepsilon_i+4\varepsilon}{k_i-k}+\frac{(\varepsilon_i+8\varepsilon)\varepsilon}{(\varepsilon_i-\varepsilon)k_i}\right\}=\Phi_h(\phi). \tag{31}$$

Comparing Eq. (29) with Eq. (31) and simplifying, one gets the following expression for e_h:

$$e_h=(1-\phi)\overline{L}_E\overline{L}_S^h(e_{hm}-e_{hi})+\left\{1+(\varepsilon_i-\varepsilon)\times\left[\frac{\varepsilon_i+4\varepsilon_m}{(\varepsilon_i+2\varepsilon_m)^2}\overline{L}_S^h-\frac{\varepsilon_i+4\varepsilon}{(\varepsilon_i+2\varepsilon)^2}\right]+\frac{k_i-k}{k_i}\left[\frac{(\varepsilon_i+8\varepsilon_m)\varepsilon_m}{(\varepsilon_i+2\varepsilon_m)^2}\overline{L}_E-\frac{(\varepsilon_i+8\varepsilon)\varepsilon}{(\varepsilon_i+2\varepsilon)^2}\right]\right\}e_{hi}, \tag{32}$$

where $\overline{L}_E$ and $\overline{L}_S^h$ are defined by Eqs. (7) and (13), respectively. It is noted that, in the special case where only the matrix phase is polarized ($e_{hi}=0$), Eq. (32) is the same as the e_h expression in Eqs. (11).

To derive the expressions for d's and other e coefficients, we need to find an expression for e_s first. The derivation of

TABLE I. Properties of constituents for PZT/PVDF 0–3 composites.

	ε[a]	Y[b] (GPa)	ν	d_{33} (pC/N)	$-d_{31}$[a] (pC/N)
PZT	1900	36	0.3	450	180
PVDF	14	1.3	0.4	0	0

[a]Reference 22.
[b]Reference 2.

TABLE II. Properties of constituents for PZT/P(VDF-TrFE) 0–3 composites.

	ε[a]	Y[b] (GPa)	ν[c]	d_{33}[a] (pC/N)	$-d_{31}$ (pC/N)
PZT	1116	71[b]	0.31[b]	410	175
P(VDF-TrFE)	9.5	1.4[c]	0.392[c]	−37	−16

[a]Reference 23.
[b]Reference 29.
[c]Reference 30.

e_s is the same as for e_h, but now all elastic moduli [starting from Eq. (26)] should be interpreted as shear moduli. Again adopt the rigidity assumption of $\mu_i \gg \mu_m$. Equation (32) may be directly rewritten for e_s as

$$e_s=(1-\phi)\overline{L_E}\,\overline{L_S^s}(e_{sm}-e_{si}) + \left\{1+(\varepsilon_i-\varepsilon)\left[\frac{\varepsilon_i+4\varepsilon_m}{(\varepsilon_i+2\varepsilon_m)^2}\overline{L_S^s}-\frac{\varepsilon_i+4\varepsilon}{(\varepsilon_i+2\varepsilon)^2}\right] + \frac{\mu_i-\mu}{\mu_i}\left[\frac{(\varepsilon_i+8\varepsilon_m)\varepsilon_m}{(\varepsilon_i+2\varepsilon_m)^2}\overline{L_E}-\frac{(\varepsilon_i+8\varepsilon)\varepsilon}{(\varepsilon_i+2\varepsilon)^2}\right]\right\}e_{si}, \tag{33}$$

where $\overline{L_S^s}$ is given by Eqs. (13).

D. Effective piezoelectric coefficients d_h, e_{31}, e_{33}, d_{31} and d_{33}

Piezoelectric strain coefficient d_h can be obtained from e_h through relations given by Eqs. (1). For piezoelectric coefficients e_{31}, e_{33}, d_{31} and d_{33}, they can be calculated from the results of Eqs. (32) and (33). The relations for such transformations for elastically isotropic materials are

$$d_h=e_h/(3k), \tag{34}$$

$$e_{31}=(e_h-e_s)/3, \tag{35}$$

$$e_{33}=(e_h+2e_s)/3, \tag{36}$$

$$d_{31}=\frac{1}{3}\left(\frac{e_h}{3k}-\frac{e_s}{2\mu}\right), \tag{37}$$

$$d_{33}=\frac{1}{3}\left(\frac{e_h}{3k}+\frac{e_s}{\mu}\right). \tag{38}$$

III. DISCUSSION

Theoretical predictions based on the foregoing expressions are compared with experimental data of Furukawa[22] for d_{31} of PZT/PVDF, and experimental data of Ng *et al.*[23] for d_{33} of PZT/P(VDF-TrFE) composites. In the latter set, there are three groups of d_{33} data that correspond to different poling conditions: only the ceramic phase is polarized (group I); both the ceramic and copolymer phases are polarized in the same direction (group II); the ceramic and copolymer phases are polarized in opposite directions (group III).

A. Effective permittivity and elastic moduli of the composites

Theoretical predictions given by Eqs. (32) and (34)–(38) require the values of the permittivity, bulk modulus and shear modulus of the composite. Sometimes the dielectric and elastic properties of the composite are not measured together with the piezoelectric properties. In such cases, we follow the same technique as that used in our previous article.[7] For the effective permittivity ε, the Bruggeman formula[25] [Eq. (A4)] is used. For the effective bulk modulus k,

$$k=k_m+\frac{\phi(k_i-k_m)}{1+(1-\phi)(k_i-k_m)/(k_m+4\mu_m/3)} \tag{39}$$

gives a good approximation for a composite with spherical inclusions.[26] For the effective shear modulus μ, explicit bounds are used. Following the work of Christensen,[27] the lower bound μ_l,

$$\mu_l=\mu_m \times\left\{1+\frac{15(1-\nu_m)(\mu_i/\mu_m-1)\phi}{7-5\nu_m+2(4-5\nu_m)[\mu_i/\mu_m-(\mu_i/\mu_m-1)\phi]}\right\}, \tag{40}$$

given by Hashin and Shtrikman[28] for arbitrary phase geometry is adopted in our prediction. In Eq. (40), ν_m is the Poisson ratio of the matrix phase. We adopt for the upper bound μ_u Hashin's formula for spherical inclusion geometry,[26] which may be rewritten as

$$\mu_u=\mu_m\left[1+\left(\frac{\mu_i}{\mu_m}-1\right)\frac{\beta}{\alpha+\beta\gamma}\phi\right], \tag{41}$$

where

$$\alpha=\frac{42}{5\mu_m}\frac{\mu_m-\mu_i}{1-\nu_m}\phi(\phi^{2/3}-1)^2,$$
$$\beta=[(7-10\nu_i)-(7-10\nu_m)\vartheta]4\phi^{7/3}+4(7-10\nu_m)\vartheta,$$
$$\gamma=\frac{\mu_i}{\mu_m}+\frac{7-5\nu_m}{15(1-\nu_m)}\left(1-\frac{\mu_i}{\mu_m}\right)+\frac{2(4-5\nu_m)}{15(1-\nu_m)}\left(1-\frac{\mu_i}{\mu_m}\right)\phi, \tag{42}$$
$$\vartheta=\frac{(7+5\nu_i)\mu_i+4(7-10\nu_i)\mu_m}{35(1-\nu_m)\mu_m}.$$

Since the effective shear modulus contains upper bound μ_u and lower bound μ_l, each prediction of d_{31} and d_{33} coefficients [Eqs. (37) and (38), respectively] gives a pair of predicted lines.

In comparing theoretical predictions with experimental data, the elastic, dielectric and piezoelectric properties of the constituent materials are needed. However, usually not all relevant properties are measured in published articles, thus typical values have been adopted in our calculation. We have used the same set of constituent properties, listed in Table I,

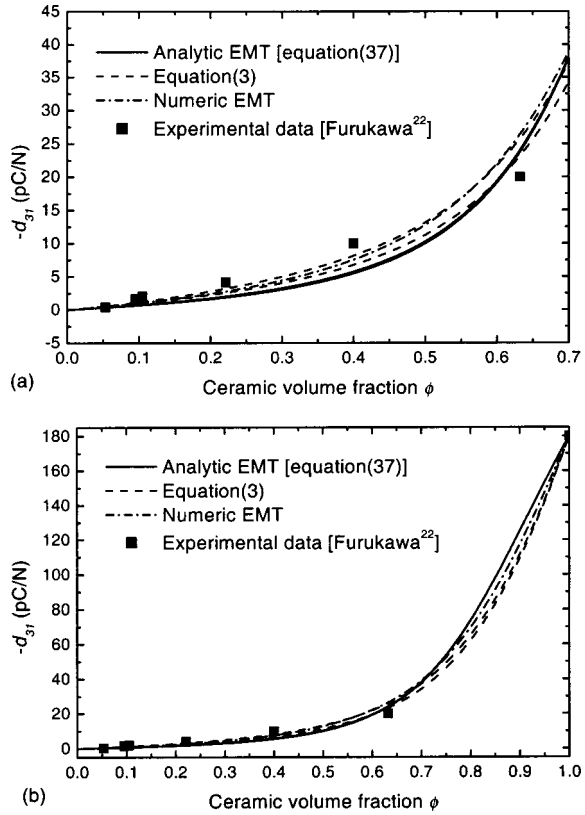

FIG. 1. Comparison of theoretical predictions of analytic EMT, Eq. (3) and numeric EMT with the experimental data of Furukawa (see Ref. 22) for the d_{31} constant of PZT/PVDF composites. (a) Only $\phi<0.7$ is shown; (b) full scale of ϕ is shown.

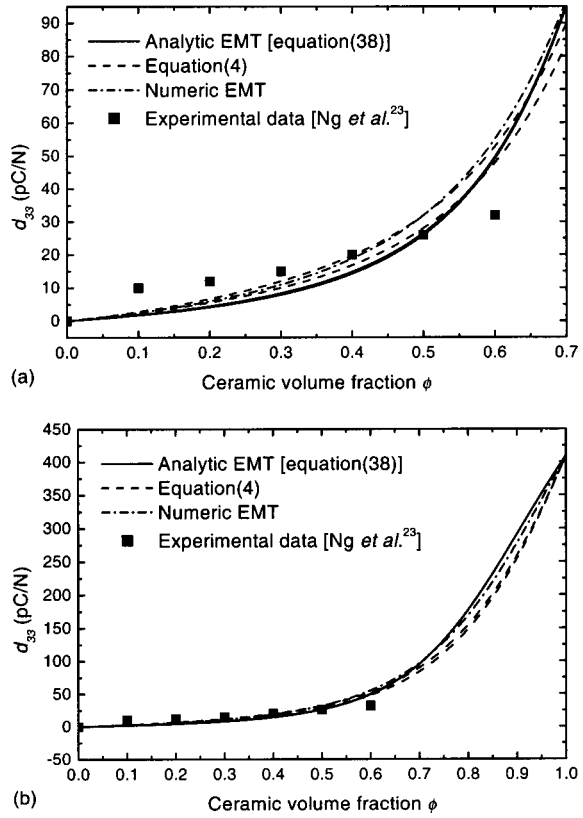

FIG. 2. Comparison of theoretical predictions by analytic EMT, Eq. (4) and numeric EMT with the experimental data of Ng *et al.* (see Ref. 23) for the d_{33} constant of PZT/P(VDF-TrFE) composites with the ceramic phase polarized. (a) Only $\phi<0.7$ is shown; (b) full scale of ϕ is shown.

as in our previous article,[7] for the prediction of Furukawa's experimental data. For the PZT/P(VDF-TrFE) system given by Ng *et al.*,[23] we assume that the Young's modulus Y_i is 71 GPa and the Poisson ratio ν_i is 0.31 for the inclusion,[29] since the ceramic powder is PKI502 from Piezo Kinetics (Bellefonte, PA).[23] With regard to the P(VDF-TrFE) copolymer, we assume that the elastic properties are similar to those given by Marra *et al.*,[30] and that $Y_m=1.4$ GPa and $\nu_m=0.392$ are used. Other constituent properties are listed in Table II.

B. Comparison with experimental data

Figure 1 shows a comparison of the theoretical predictions of EMT and Eq. (3) with the d_{31} values from Furukawa's experiment. Good agreement with the experimental data was obtained. Figure 2 shows a similar comparison with the d_{33} values for Ng *et al.*'s group I composites (only the ceramic phase is polarized). Our predictions are smaller than the experimental values for $\phi<0.4$ but larger at $\phi=0.6$. Theoretical predictions were obtained from the analytic EMT [Eq. (37) for d_{31} and Eq. (38) for d_{33}] and numerically (obtained by numeric integration without making rigidity approximations). In Figs. 1 and 2, the pair of predicted lines given by the analytic EMT were shown to nearly overlap each other. Both Figs. 1(a) and 2(a) reveal that the predicted lines from analytic EMT are only slightly displaced from those of numeric EMT. If the results given by numeric EMT are taken as ''exact'' predictions based on EMT, we can conclude that the analytic EMT scheme is a good approximation. As shown in Figs. 1(b) and 2(b), the resulting lines [Eqs. (37) and (38)] deviated more from numeric EMT as ϕ increases. However, we notice that those larger deviations occur only when $\phi>0.6$. Actually, it becomes quite difficult to fabricate 0–3 composite samples with such high ceramic volume fractions. It is clear that all predicted lines are very close to each other for $\phi<0.6$. Therefore we believe that Eqs. (37) and (38) give reasonable predictions for $\phi<0.6$. In our previous paper,[7] we gave expressions for effective d_{31} and d_{33} coefficients [Eqs. (3) and (4)] that cover both dilute and concentrated suspensions. These predictions for concentrated suspensions have also been shown in Figs. 1 and 2 for comparison, but the pair of predicted ''bounds'' are not as close to each other as in the analytic EMT scheme. We also found that the predictions of numeric EMT always lie between the pair of lines predicted by Eqs. (3) and (4).

Continuing with Ng *et al.* data, Fig. 3 shows a comparison with the d_{33} values of group II composites (both phases are polarized in the same direction). The comparison shows that our predictions agree quite well with the experimental values. Figure 3 also shows the theoretical predictions given by Nan and Weng[10] who used an effective medium approach to obtain numerical results for group II and group III samples of Ng *et al.*'s experimental data. Figure 3 shows that Nan and Weng's predictions deviate quite significantly from the experimental data at higher inclusion volume fractions. From Fig. 3(b), it should be noted that Nan and Weng have as-

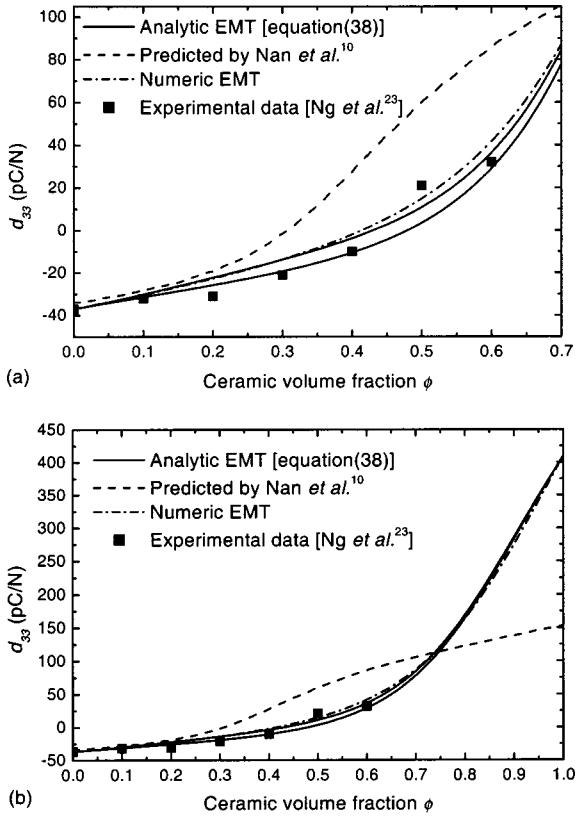

FIG. 3. Comparison of the theoretical predictions by analytic EMT, Nan and Weng, and numeric ENT with the experimental data of Ng *et al.* (see Ref. 23) for the d_{33} constant of PZT/P(VDF-TrFE) composites with the ceramic and copolymer phases polarized in the same direction. (a) Only $\phi<0.7$ is shown; (b) full scale of ϕ is shown.

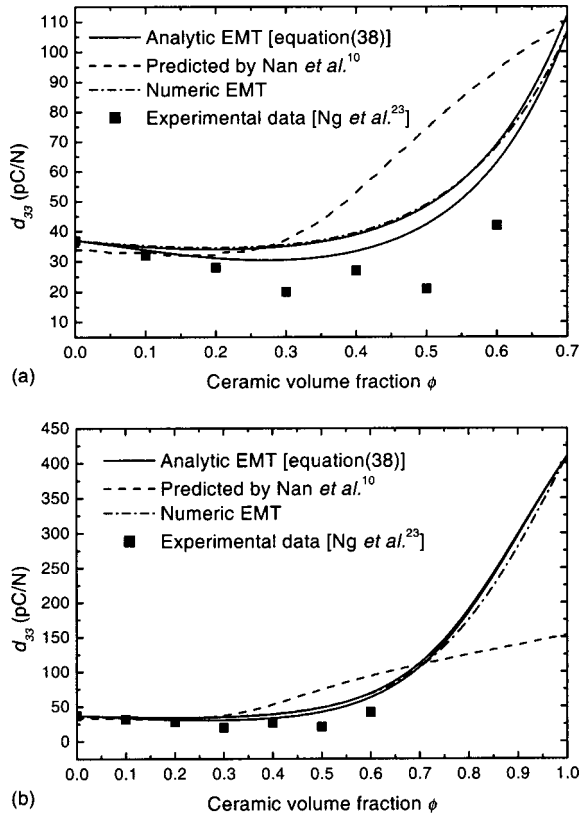

FIG. 4. Comparison of the theoretical predictions by analytic EMT, Nan and Weng, and numeric EMT with the experimental data of Ng *et al.* (see Ref. 23) for the d_{33} constant of PZT/P(VDF-TrFE) composites with the ceramic and copolymer phases polarized in opposite directions. (a) Only $\phi<0.7$ is shown; (b) full scale of ϕ is shown.

sumed that $d_{33i}=153$ pC/N. Moreover, they adopted inclusion permittivities of $\varepsilon_{11}=450$ and $\varepsilon_{33}=235$, which are significantly lower than those measured by Ng *et al.* (see Table II).

Figure 4 shows a comparison with the d_{33} values of group III composites (both the ceramic and copolymer are polarized, but in opposite directions). Both Nan and Weng's predictions and our predictions shown are larger than the experimental values. The discrepancy between prediction and the experimental data is most likely due to the fact that the composite samples are difficult to fully pole.[23] We believe that this effect is more readily observable in composite samples with phases poled in the opposite directions, as will be explained later. An insufficient degree of poling of the constituent material results in a lower value of remanent polarization after poling, hence less piezoelectric activity (with respect to that in the fully poled material). The piezoelectric coefficients of the ceramic and copolymer phases have opposite signs; their piezoelectric activities should reinforce each other when these phases are polarized in opposite directions. For such composite samples, if they are not fully poled, the piezoelectric coefficients of the composites will always be lower than that of the fully poled samples (as shown in Fig. 4, the experimental data are lower than the prediction which assumes complete polarization). The degree of poling of the constituent material depends on the poling procedure. A further important consideration is how the poling procedure affects the degree of poling. Ng *et al.*'s composite samples with oppositely polarized phases were obtained by applying, as the final poling step, a constant poling field on the composite sample in the direction opposite the polarization of the pre-polarized ceramic phase for half an hour;[23] the intent was to pole the copolymer phase. For a high poling field in this step, the initial polarization in the ceramic phase will be reduced or even switched to the direction of the field applied. On the other hand, for a low poling

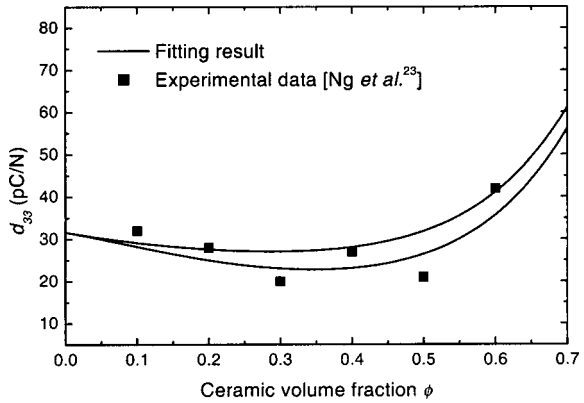

FIG. 5. Mathematical fit to the experimental data of Ng *et al.* (see Ref. 23) for the d_{33} constant using Eqs. (32), (33), (37), (38) and (43). The ceramic and copolymer phases in the PZT/P(VDF-TrFE) composites are polarized in opposite directions.

TABLE III. Relative width of the predicted lines by Eqs. (9), (3) and (4) with adopted properties of the constituents shown in Table II.

	Maximum $\mathfrak{R}^a$ ($\times 10^{-2}$)			ϕ
	$\mathfrak{R}_s$	$-\mathfrak{R}_{31}$	$\mathfrak{R}_{33}$	at max $\mathfrak{R}$
(A) Only the ceramic phase is polarized	1.64	1.83	1.56	0.78
(B) Only the matrix phase is polarized	19.19	21.19	18.32	0.55
(C) Two phases polarized in the same direction	2.86	3.18	2.72	0.7
(D) Two phases polarized in opposite directions	−0.9	−1	−0.86	0.38

[a]Largest magnitude of $\mathfrak{R}$.

field, the degree of poling in the copolymer phase will be limited. For this reason, we believe that an optimal degree of poling in samples with oppositely polarized phases is difficult to achieve with this poling procedure. Thus for our analysis of the experimental data we assume that the copolymer phases in all group III composites have roughly the same degree of poling and that similar assumption can be made for the ceramic phases. Then an estimate of the reduction in piezoelectric activity (with respect to values for fully poled material) in the constituents may be obtained by fitting the experimental data. We define the degree of poling $\mathcal{I}$ by

$$\mathcal{I}_i \equiv d_{33i}/d_{33i}^f = d_{31i}/d_{31i}^f,$$
$$\mathcal{I}_m \equiv d_{33m}/d_{33m}^f = d_{31m}/d_{31m}^f, \tag{43}$$

where the superscript f denotes ''fully poled.'' Using Eqs. (32), (33), (37), (38) and (43) and the fully poled d values given in Table II, a reasonable fit to the experimental data is shown in Fig. 5. The fitting result gives $\mathcal{I}_i = 0.49$ and $\mathcal{I}_m = 0.85$. Although these values need not be identical to ''true values'' of the degree of poling, it still reflects that the degree of poling in the inclusion phase is significantly lower than that in the matrix phase. This result suggests a reduction of the initial polarization in the ceramic phase due to the final poling step. On the other hand, the fitting result gives $d_{33i} \approx 200$ pC/N which comes closer to the value used by Nan and Weng ($d_{33i} = 153$ pC/N). However, their justification was based on the assumption that the properties of the PZT phase were similar to those of PZT-7A.[10]

C. ''Bound width'' comparison of analytic EMT with Eqs. (3), (4) and (9)

Because the prediction of d_{31} or d_{33} gives a pair of lines, their ''width'' may dictate their applicability for meaningful predictions and generally narrower bounds are preferred. We mentioned earlier that the pair of predicted lines for the analytic EMT scheme is closer to each other than those predicted by Eqs. (3) and (4) (Figs. 1 and 2). This will be discussed further here in Sec. III C. We first define the relative width $\mathfrak{R}$ for a pair of predicted lines:

$$\mathfrak{R}_s(\phi) \equiv [d_{s,u}(\phi) - d_{s,l}(\phi)]/[\text{maximum } d_s - \text{minimum } d_s],$$
$$\mathfrak{R}_{31}(\phi) \equiv [d_{31,u}(\phi) - d_{31,l}(\phi)]/[\text{maximum } d_{31} - \text{minimum } d_{31}], \tag{44}$$
$$\mathfrak{R}_{33}(\phi) \equiv [d_{33,u}(\phi) - d_{33,l}(\phi)]/[\text{maximum } d_{33} - \text{minimum } d_{33}],$$

where d with subscripts u and l denotes d calculated with μ_u and μ_l, respectively. It is also worthwhile to investigate d_s, since the shear modulus is the only elastic parameter involved in Eq. (9). On the other hand, Eq. (9) can be reduced to the familiar d coefficient expression given by Furukawa *et al.*,[2] by using Eqs. (40), with $\nu_i = \nu_m = 0.5$, and (A1). Using the properties of constituents in Table II, $\mathfrak{R}_s$, $\mathfrak{R}_{31}$ and $\mathfrak{R}_{33}$ can be calculated through Eqs. (9), (3) and (4) or the analytic EMT scheme. All $\mathfrak{R}$'s are functions of ϕ. Table III shows the maximum $\mathfrak{R}$ (largest magnitude) values, along with the ϕ values at which maximum $\mathfrak{R}$ occur for the different poling conditions [cases (A)–(D)], calculated from Eqs.

TABLE IV. Relative width of the lines predicted by the analytic EMT scheme with adopted properties of the constituents shown in Table II.

	Maximum $\mathfrak{R}^a$ ($\times 10^{-2}$)			ϕ
	$\mathfrak{R}_s$	$-\mathfrak{R}_{31}$	$\mathfrak{R}_{33}$	at max $\mathfrak{R}$
(A) Only the ceramic phase is polarized	0.17	0.19	0.16	0.55
(B) Only the matrix phase is polarized	19.19	21.19	18.32	0.55
(C) Two phases polarized in the same direction	1.75	1.95	1.66	0.55
(D) Two phases polarized in opposite directions	1.69	1.88	1.61	0.55

[a]Largest magnitude of $\mathfrak{R}$.

(9), (3) and (4). Values in Table IV, in contrast, are obtained from the analytic EMT scheme. When only the ceramic phase is polarized [case (A)], the $\Re$'s for both schemes are generally small and the pair of predicted lines are very close to each other. However, bounds for the analytic EMT scheme are very narrow with both lines nearly coinciding with each other (Figs. 1 and 2). For composites with only the matrix phase polarized [case (B)], both schemes give identical predictions and the relative width of the bounds constitutes about 20% of the full scale range, which suggests the present models may not be too useful for such predictions. Nevertheless, no experimental data are available for the present case under investigation. Concerning both phases polarized in the same direction [case (C)], the analytic EMT scheme also gives closer bounds than the other scheme, but both schemes show bounds that are slightly wider than in case (A) (cf. Figs. 2 and 3). This is because the predicted values for this case are essentially a linear combination of the conditions for cases (A) and (B). Since the predicted lines for case (B) are far apart, predictions for those for case (C) are expected to be further apart than for case (A). However, for case (D) in which both phases are polarized in opposite directions, the predicted values are the difference in conditions for cases (A) and (B). The resultant width of the bounds, as well as the sign of $d_u(\phi)-d_l(\phi)$, depends on the difference of the width of bounds for cases (A) and (B). In the experimental system of Ng *et al.*,[23] the predictions by the analytic EMT give $d_u(\phi)>d_l(\phi)$, but the predicted lines by Eqs. (9), (3) and (4) show $d_u(\phi)<d_l(\phi)$ for $\phi<0.71$ and $d_u(\phi)>d_l(\phi)$ elsewhere which looks strange (i.e., $\Re<0$ in Table III). Tables III and IV also reveal $\phi=0.55$ at maximum $\Re$ for all poling conditions using the analytic EMT scheme, but this is not so for the scheme using Eqs. (9), (3) and (4). Based on the above analysis, the analytic EMT scheme seems to be the preferred choice for fitting the experimental system of Ng *et al.*

In case the predicted lines are not close enough to give a good estimate of the piezoelectric coefficients [such as in case (B) in the present system], a single expression (instead of bounds) for the effective shear modulus like that provided by Au *et al.*[21] may be employed. Such estimations will be higher than in the present scheme, especially for ϕ exceeding 70%. This is not surprising since Au *et al.*'s expressions assume rigid inclusions.

IV. CONCLUSIONS

Based on the expressions of effective piezoelectric stress coefficients $e_h(\equiv e_{33}+2e_{31})$ and $e_s(\equiv e_{33}-e_{31})$ for ferroelectric 0–3 composites of small inclusion volume fractions, explicit expressions of such coefficients for the nondilute case were derived using an effective medium theory. New sets of explicit expressions for d_h, d_{33}, d_{31}, e_{33} and e_{31} coefficients can also be calculated from e_h and e_s. These expressions involve the dielectric and elastic properties of the composite, which can be evaluated by the Bruggeman formula and Hashin bounds. Analytical predictions were compared with the numeric EMT scheme for the experimental results of PZT/PVDF and PZT/P(VDF-TrFE) given by Furukawa[22] and by Ng *et al.*,[23] respectively. The comparison showed that the predictions of analytic EMT expressions are very close to the numeric EMT scheme for $\phi<0.6$, even though the elastic moduli of the inclusion phase were assumed to be very large for the analytic EMT scheme. Fairly good agreement with the experimental values was also achieved. The discrepancies in the predictions with the experimental data of samples with oppositely polarized constituents were examined and it is suggested that the origin is the low degree of poling, due especially to the reduction of initial polarization in the ceramic phase. In addition, analysis of bounds for the predicted lines were performed. The analytic EMT scheme shows advantages over the previous scheme on the experimental system of Ng *et al.*

ACKNOWLEDGMENT

This work was supported by a Center for Smart Materials of Hong Kong Polytechnic University research grant.

APPENDIX

Consider the characteristic equation [Eq. (17)] that relates ϕ and ε as well as the Maxwell–Wagner formula:[24]

$$\varepsilon=\frac{\varepsilon_i+2\varepsilon_m+2\phi(\varepsilon_i-\varepsilon_m)}{\varepsilon_i+2\varepsilon_m-\phi(\varepsilon_i-\varepsilon_m)}\varepsilon_m. \tag{A1}$$

Eqs. (17) and (A1) yield

$$\frac{d(1-\phi)}{1-\phi}=\left(\frac{1}{3\varepsilon_m}+\frac{1}{\varepsilon_i-\varepsilon_m}\right)d\varepsilon_m. \tag{A2}$$

Thus the first integral is

$$S(\phi)=(1-\phi)\frac{\varepsilon_i-\varepsilon_m}{\varepsilon_m^{1/3}}. \tag{A3}$$

Hence $S(0)=(\varepsilon_i-\varepsilon_m)\ \varepsilon_m^{-1/3}$. We can further write $(\varepsilon_i-\varepsilon)\varepsilon^{-1/3}=S(\phi)$. Comparing this with Eq. (A3), one gets the Bruggeman formula:[25]

$$\frac{\varepsilon_i-\varepsilon}{\varepsilon^{1/3}}=(1-\phi)\frac{\varepsilon_i-\varepsilon_m}{\varepsilon_m^{1/3}}. \tag{A4}$$

[1] T. Yamada, T. Ueda, and T. Kitayama, J. Appl. Phys. **53**, 4328 (1982).
[2] T. Furukawa, K. Ishida, and E. Fukada, J. Appl. Phys. **50**, 4904 (1979).
[3] N. Jayasundere, B. V. Smith, and J. R. Dunn, J. Appl. Phys. **76**, 2993 (1994).
[4] M. L. Dunn and M. Taya, Int. J. Solids Struct. **30**, 161 (1993).
[5] B. Jiang, D. N. Fang, and K. C. Hwang, Int. J. Solids Struct. **36**, 2707 (1999).
[6] C. K. Wong, Y. M. Poon, and F. G. Shin, Ferroelectrics **264**, 39 (2001).
[7] C. K. Wong, Y. M. Poon, and F. G. Shin, J. Appl. Phys. **90**, 4690 (2001).
[8] C. W. Nan, J. Appl. Phys. **76**, 1155 (1994).
[9] C. W. Nan and D. R. Clarke, J. Am. Ceram. Soc. **80**, 1333 (1997).
[10] C. W. Nan and G. J. Weng, J. Appl. Phys. **88**, 416 (2000).
[11] H. Zewdie, Bull. Chem. Soc. Ethiopia **12**, 159 (1998).
[12] D. Stroud, Superlattices Microstruct. **23**, 567 (1998).
[13] M. Avellaneda and T. Olson, J. Intell. Mater. Syst. Struct. **4**, 82 (1993).
[14] T. C. Choy, *Effective Medium Theory: Principles and Applications* (Oxford University Press, New York, 1999).
[15] K. W. Yu, Solid State Commun. **105**, 689 (1998).
[16] F. G. Shin, W. L. Tsui, and Y. Y. Yeung, J. Mater. Sci. Lett. **8**, 1383 (1989).
[17] F. G. Shin, Y. Y. Yeung, and W. L. Tsui, J. Mater. Sci. Lett. **9**, 948 (1990).
[18] F. G. Shin, Y. Y. Yeung, and W. L. Tsui, J. Mater. Sci. Lett. **9**, 1002 (1990).

[19] F. G. Shin, W. L. Tsui, and Y. Y. Yeung, J. Mater. Sci. Lett. **12**, 1163 (in Chinese) (1993).
[20] R. McLaughlin, Int. J. Eng. Sci. **15**, 237 (1977).
[21] W. M. Au, W. L. Tsui, and F. G. Shin, Acta Mater. Compos. Sin. **11**, 49 (1994).
[22] T. Furukawa, IEEE Trans. Electr. Insul. **24**, 375 (1989).
[23] K. L. Ng, H. L. W. Chan, and C. L. Choy, IEEE Trans. Ultrason. Ferroelectr. Freq. Control **47**, 1308 (2000).
[24] J. C. Maxwell, *A Treatise on Electricity and Magnetism* (Dover, New York, 1954) (reprint).
[25] D. A. Bruggeman, Ann. Phys. (Leipzig) **24**, 636 (1935).
[26] Z. Hashin, J. Appl. Mech. **29**, 143 (1962).
[27] R. M. Christensen, *Mechanics of Composite Materials* (Wiley, New York, 1979), Chap. 4.
[28] Z. Hashin and S. Shtrikman, J. Mech. Phys. Solids **11**, 127 (1963).
[29] Data sheet from Piezo Kinetics Inc.
[30] S. P. Marra, K. T. Ramesh, and A. S. Douglas, Compos. Sci. Technol. **59**, 2163 (1999).